Multi-level Land Cover Mapping of the Twin Cities (Minnesota) Metropolitan Area with Multi-seasonal Landsat TM/ETM+ Data

Fei Yuan, Marvin E. Bauer, Nathan J. Heinert, and Geoffrey R. Holden

Preprint of Paper Accepted for Publication in Geocarto International (In Press, 2005)

Fei Yuan (Corresponding author)
Research Assistant
Remote Sensing and Geospatial Analysis Laboratory
College of Natural Resources
University of Minnesota
1530 N. Cleveland Avenue
St. Paul, Minnesota 55108 USA
Phone: 612-624-3459
Email: yuan0024@umn.edu

Marvin E. Bauer
Professor, Remote Sensing
College of Natural Resources
University of Minnesota
1530 N. Cleveland Avenue
St. Paul, Minnesota 55108 USA
Phone: 612-624-3703
Email: mbauer@umn.edu

Nathan J. Heinert
Meteorologist
National Weather Service
1945 Beechcraft Avenue
Pocatello, Idaho 83204 USA

Geoffrey R. Holden
Forester
USDA North Central Research Station
1992 Folwell Avenue
St. Paul, Minnesota 55108 USA

Multi-level Land Cover Mapping of the Twin Cities (Minnesota) Metropolitan Area with Multi-seasonal Landsat TM/ETM+ Data

Abstract

Land cover maps, especially vegetation maps, are of increasing interest and use to resource agencies. This paper describes a three-stage hybrid classification method for regional-scale multi-level land cover mapping. The first stage involves an unsupervised classification and stratification. The second stage includes supervised classification of forest types, rule-based clustering of non-forested vegetation, and estimation of percent impervious area with a regression model. The third stage is final map generation and post processing. Landsat TM/ETM+ images of three (spring, summer, fall) dates were used to classify land cover of the seven-county Twin Cities Metropolitan Area of Minnesota into three levels of the modified Minnesota Land Cover Classification System. The overall accuracies for Level-1 and Level-2 classes were 95% and 89%, respectively, and the agreement between the estimation of percent impervious surface in Level-3 classification and the measurements from digital ortho photographs was 96%.

Introduction

Land use and land cover is regarded as the single most important factor of environmental change such as deforestation, habitat fragmentation, urbanization, and wetland degradation (Turner et al., 1995; Lunetta et al., 2002). Timely and accurate information on existing land use and land cover are required by decision makers and scientists at all levels. Land use and land cover inventories could be done from field survey or interpretation of large-scale aerial photography, but both are time consuming and expensive. Satellite remote sensing provides a more practical way to map and monitor land cover, especially over large geographic areas.

Some studies have shown the possibility of mapping broad-scale land cover to more specific levels using Landsat Thematic Mapper (TM) imagery. For example, Ma et al. (2001) demonstrated a two-stage classification for mapping vegetation across large geographic areas with TM imagery and multi-source ancillary data. Reese et al. (2002) described a process for deriving statewide land cover from multi-seasonal TM data. However, the majority of research has been focused on land cover mapping of USGS Level-1 or -2 classes due to the relatively low resolution of TM data, although broad-scale land cover maps, especially vegetation with Level-3 classes, are also of interest (Anderson, 1976). Ideally, more detailed Level-3 classes may be inventoried using data with higher spatial resolution such as digital ortho photographs (DOQs) or IKONOS imagery (Welch, 1982; Stefanov et al., 2001). But this is only cost effective when the study area to be mapped is fairly small (Mumby and Edwards, 2002).

Several projects on classification of Landsat TM data of the Twin Cities Metropolitan Area (TCMA) of Minnesota have demonstrated that it is possible to achieve overall classification accuracies of 90% for general (Level-1) land cover classes (agricultural, forests, wetland, water, and urban) classes, and approximately 80% for Level-2 classes (Sawaya, et al., 2001). A variety of image classification methods including maximum-likelihood, guided clustering, contextual, artificial neural network and knowledge-based classifications have been utilized in previous land cover studies of this area (Bauer et al., 1994; Bauer et al. 1996; Özesmi, 2000; Stukens et al., 2000). Additionally, a strong relationship in the Landsat data to impervious surfaces that can be used to map percent impervious surface area was also found (Bauer et al., 2004).

Based on the results of previous research, a multi-stage three-level hierarchical classification method was defined and accomplished in this study. This paper describes the methods and results of classifications of multi-temporal Landsat TM/ETM+ data covering the seven-county TCMA. The classifications are of imagery acquired in 2000 and include three levels of specificity of land cover type, including percent impervious surface area for the urban/developed classes. The objectives were: (1) to extend land cover classification in TCMA into multiple level classes of the Minnesota Land Cover Classification System (MLCCS); (2) to explore the use of multi-temporal imagery made possible by the availability of two Landsat satellites.

2. Methods

2.1 Study Area

The study area is the Twin Cities Metropolitan Area (TCMA) of Minnesota. It includes Anoka, Carver, Dakota, Hennepin, Ramsey, Scott, and Washington counties, with an area of approximately 7700km^2 (Figure 1). Physically, it is divided into four physiographic strata – northern Anoka Sand Plain, Eastern St. Croix Moraine, southern Rochester Till Plain and western Owatanna Moraine (Wright, 1972). Land covers in the area are quite diverse with high density and low density urban dominating the central part, and several rural land covers including cropland, grassland, wetland, and forest in the surrounding areas. Crop production is a leading endeavor in the rural areas. Major forest types include aspen, oak, white pine, and red pine. Land cover in TCMA has undergone dramatic changes over the last several decades due to rapid urban developments. The population of the TCMA increased 15.4% (from 2.29 million to 2.64 million) from 1990 to 2000.

2.2. Landsat TM/ETM+ Data and Preprocessing

Multi-seasonal Landsat TM/ETM+ images acquired in the spring, summer, and fall 2000 were obtained from the EROS Data Center. For each date, two images corresponding to Landsat path 27, rows 28 and 29, which covers our study area were

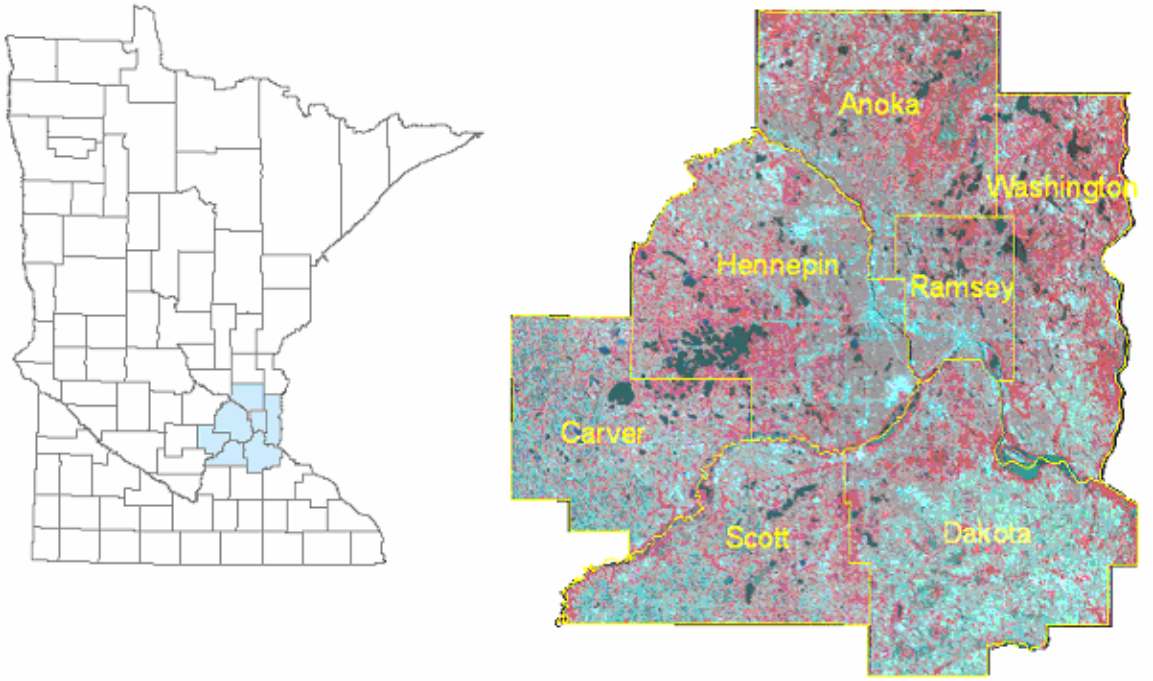

Figure 1. Seven-county Twin Cities Metropolitan Area of Minnesota and June 8, 2000, Landsat TM, false color composite (RGB = bands 4, 3, 2).

acquired. All of the images were free of clouds and haze. Multi-temporal imagery produces higher classification accuracy than that can be obtained from a single date image (Coppin and Bauer, 1994; Wolter et al., 1995). Reese et al. (2002) demonstrated that higher classification accuracy can be obtained in areas with forest and agriculture cover types when using three dates of imagery acquired in spring, summer, and fall from the same year. All the images were georeferenced to a May 1998 Landsat image, which was originally rectified to the Minnesota Department of Transportation (DOT) basemap with an overall RMS less than 7.5 meters. Each image was rectified using 50-60 ground control points (GCPs) evenly distributed across the entire image. The GCPs selected included road-intersections, some structure corners, and field boundaries. All the rectified images were projected to the UTM system, Spheroid GRS 1980, Zone 15 North, Datum GRS 1980. Table 1 lists the detailed information for the three dates of images. After projection, the two scenes from the same date were mosaiced and then clipped to match the boundary of the entire TCMA and "stacked" into a 21-band image file.

Table 1. Acquisition dates and rectification information of Landsat imagery.

Acquisition Date	Sensor	Number GCPs	RMS Error (m)
April 29, 2000	ETM+	65	7.5
June 8, 2000	TM	50	7.2
September 12, 2000	TM	52	8.5

2.3. Ancillary and Field Data

Ancillary data have been widely shown to help discrimination of classes that are difficult to classify using remotely sensed data itself (Brown et al., 1993; Foody, 1995; McIver and Friedl, 2002). In this study, ancillary data from several sources, the Metropolitan Council 2000 DOQs and 1997 land use map, 2000 base map from the Minnesota Department of Transportation (DOT), and the 1990 National Wetlands Inventory (NWI), were obtained and proved helpful to the classifications and accuracy assessment.

Another critical aspect of successfully classifying Landsat data is the availability of adequate and accurate field data that can be used to associate spectral-radiometric-temporal classes from the imagery with land cover/land use classes. The major field data for this study was the digital land cover map of Minnesota Land Cover Classification System (MLCCS) Level 1 to 4.5 provided by the Minnesota Department of Natural Resources (DNR).

2.4. Classification Scheme

The first step in any mapping or image classification project is to identify a classification scheme, a systematic listing of the classes of interest. The scheme needs to be exhaustive (there is a class for everything) and mutually exclusive (each cover type is a member of only one class). It should also be hierarchical so that detailed classes can be collapsed into more general classes. A large number of classes may lead to misclassification among cover types, while too few classes may not meet the user's information needs. In this study, it was required that the classification scheme be compatible with the existing MLCCS scheme. A three-level method (Table 2) balancing the specificity of the MLCCS with the land use and land cover classes which we believed could be classified with reasonable accuracy was adopted.

3. Classification Methodology

A flow chart summarizing the approach to image classification is shown in Figure 2. In summary, a hierarchical approach and a layered classification procedure was followed. The general processing steps listed in the flow chart and the specific steps are described in the following sections.

3.1. First Stage – Unsupervised Classification and Stratification

In the first stage, an unsupervised classification, Iterative Self-Organizing Data Analysis Technique (ISODATA), was performed on the stacked multi-temporal TM image in ERDAS Imagine. The number of clusters, maximum number of iterations, and convergence threshold was set to 100, 60, and 0.99 respectively. Using ancillary and field data as references, the 100 clusters were then analyzed and recoded into information classes such as high density urban, low density urban, cropland, wetland, grass (natural and planted), upland shrub, forest, and water. The reason and significance of this step was to check and identify the problems caused by similar spectral responses of information classes. Clusters containing more than one land cover class were identified and addressed using the rule-based spatial analysis technique described below.

Using the lowland mask generated from the NWI, wetlands were unmixed from other classes by applying the rule – the pixel in the mixed cluster was wetland (i.e., lowland) if it was in the lowland mask – in a rule-based spatial modeler generated in ERDAS Imagine. Similarly, upland grass was further separated into planted grass (mainly golf courses or lawns) and natural upland grass using a vector file that delineated the central urban boundary and surrounding towns from rural areas. The vector file was digitized on screen in the Landsat imagery overlaid with the 2000 DOT base map. The rule here was – the grass was planted if it was within the urban boundary, otherwise it was natural upland grass. Also, mixed clusters consisting of cropland (cultivated or fallow), grass, and low density urban were processed and divided using the DOQs and the DOT base map as references. This was done by digitizing the AOIs (areas of interest) of crops, grass, and low density urban for the large mixed clusters and separating these classes using the rule-based spatial modeler.

The result of the initial classification was a land cover map containing the following classes: cropland, forest, high-density urban, low-density urban, upland natural grass, upland planted grass, upland shrubland, wetland, and water. Based on this map, forest, urban and water strata were generated for further classification in the next stage.

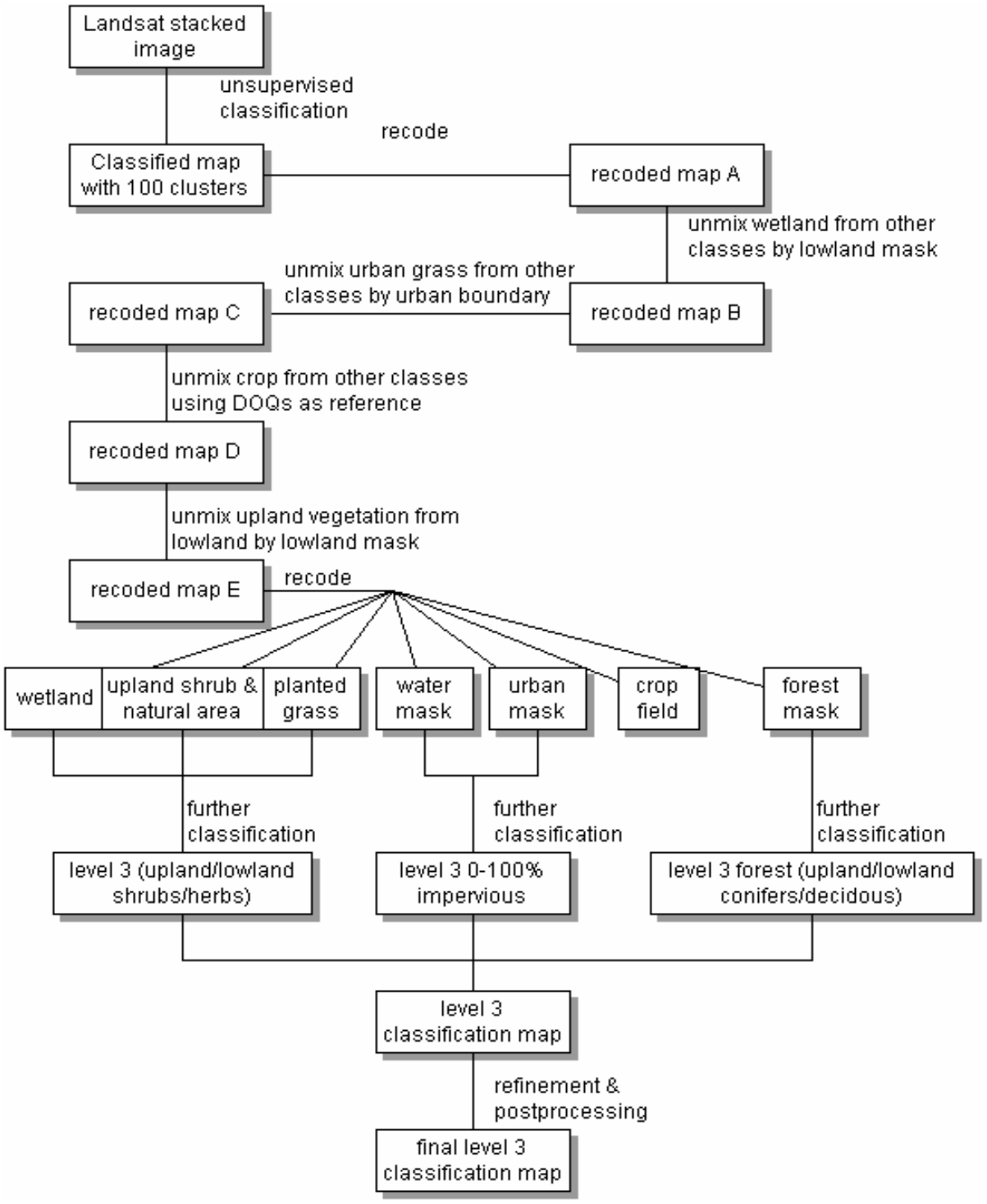

Figure 2. Major steps in the classification procedure.

Table 2. Classification scheme for Landsat classification in the TCMA.

Level- 1	Level- 2	Level- 3	Description
Urban (Artificial Surfaces)	0-4% Density 5-10% Density 11-25%Density 26-50% Density 51-75% Density 75-100% Density	0-100% Imperviousness	Level-2 urban density is based on the impervious classification.
Agriculture (Planted or Cultivated)	Cropland	Cropland	Corn, soybean, small grains, hay, pasture, etc.
	Planted trees & grasses	Planted trees, shrubs & grasses	
Forest	Coniferous	Upland conifer	White pine, red pine, eastern red cedar
		Lowland conifer	Tamarack
	Deciduous	Upland deciduous	Oak, maple-basswood, aspen, box elder, oak woodland-brush land, disturbed deciduous woodland
		Lowland deciduous	Floodplain forest, lowland hardwood, aspen forest temporarily flooded, black ash swamp, mixed hardwood swamp, aspen forest saturated
Non-forested natural area	Upland shrubland & herbaceous	Upland shrubland	Upland shrubland
		Upland herbaceous	Grassland with sparse deciduous trees, grassland with sparse conifer trees, mesic prairie-tall grasses, dry prairie-medium tall grasses Dry oak savanna, mesic oak savanna
	Lowland shrubland & herbaceous	Lowland shrubland	Temporarily flooded shrubland, alder swamp, wet meadow shrub subtype, willow swamp
		Lowland herbaceous	Wet meadow, poor fen, rich fen, cattail marsh, mixed emergent marsh
Water			

3.2. Second Stage – Level 2-3 Classifications of Forest, Urban, and Non-forested Area

3.2.1. Generation of Level 2-3 Forest Classes

To divide the forest class into conifers and deciduous, the April image was restacked to omit all bands but 3, 4, and 5 (red, near infrared, and middle infrared). This date and band combination provided the best differentiation between coniferous and deciduous species (Nelson et al., 1984; Benson and DeGloria, 1985). Using the forest mask generated in the first stage, the non-forested areas were removed from the newly stacked April image so that only the forest pixels were remained.

Training and accuracy signatures were generated using the MLCCS data provided by the DNR. Selections based on the Level-4 classes were used to incorporate as much variation as possible for the Level-2 classes. Since the data did not match directly with the imagery due to possible errors in the rectification, scale differences, and some errors in the MLCSS data, the polygons were not used directly. Instead, AOIs were created manually within the polygons. The Landsat imagery itself and DOQs were used to verify that the boundaries of the classes in question matched the AOIs. The MLCCS Level- 4 classes selected to represent the forest class were as follows: Upland coniferous forest (planted conifers); Lowland coniferous forest (tamarack); Upland deciduous forest (oak forest, aspen forest, box elder-green ash disturbed native forest, and maple-basswood forest); Lowland deciduous forest (aspen forest – saturated, aspen forest – temporarily flooded, floodplain forest); Lowland hardwood forest (mixed hardwood swamp); Woodland (disturbed deciduous woodland; oak woodland-brushland). These classes were extracted from the larger MLCCS dataset. Polygons were selected based on the following three criteria: (1) maximization of spatial distribution for each class, (2) size of polygon from which to extract signatures, and (3) good representation of spectral-radiometric variation within a class based on visual interpretation of the imagery.

Signatures that represented planted conifer, natural conifer, and natural deciduous were then grouped together into one signature file for each Level-2 class (conifer or deciduous). Next, each signature file was split into two groups – one for training the classifier and one for accuracy assessment. This split was based on a visual comparison of the variation within each Level-4 class. Image histograms and spectral plots assisted in this comparison. Finally, the training signature files for each Level-2 class were combined into a single file. Unique names based on the Level-4 classes were generated for each signature and retained throughout this step. Using the training signatures, a supervised classification was run using the maximum likelihood classification algorithm. The information classes that were identified included planted conifer, deciduous and tamarack. There was not enough reference data available to classify upland coniferous species, so tamarack was used to represent the entire coniferous class. This assumption seemed acceptable since the number of naturally occurring conifers within the TCMA is relatively small compared to tamarack. Instead, it was assumed that all upland conifers

within the TCMA were planted, and therefore, could be represented by the MLCCS class of planted conifer.

For the Level-3 classification, conifers and deciduous were further separated into upland and lowland classes. This was done using the lowland mask discussed in the first stage. The assumption was made that any conifer or deciduous located within the mask was of the lowland variety. All others were classified as upland. Essentially, three new classes were created – lowland planted conifer, lowland deciduous, and lowland tamarack. The original three classes were then labeled as upland planted conifer, upland deciduous and upland tamarack. Since, tamarack does not occur in upland areas, it was assumed that these pixels were upland deciduous that were erroneously classified. These pixels were recoded to reflect this assumption. Finally, using a polygon shapefile provided by the DNR, some upland planted conifer was recoded as upland natural conifer.

3.2.2. Generation of Level 2-3 Shrubland and Herbaceous Classes

To generate Level-2 and Level-3 shrubland and herbaceous classes, wetland from the first stage was separated using the NWI data. This was done by intersecting the wetland with the NWI Circular 39 classes using the spatial analysis modeler in ERDAS Imagine. The wetland class was divided into eight subclasses since eight Circular 39 classes (bogs, deep marsh, seasonally flooded basin, shallow marsh, shrub swamp, wet meadow, and wooded swamp) exist in the TCMA. In this project, shrub swamp, wooded swamp, and bogs were grouped into lowland shrub. Seasonally flooded basin, wet meadow, shallow marsh, and deep marsh were grouped into lowland herbaceous. This arrangement was based on the lowland shrubland and lowland herbaceous definitions in MLCCS, in which lowland shrubland refers to temporarily flooded shrub land, wet meadow shrub subtype and alder or willow swamp, while lowland herbaceous mainly includes wet meadow, wet prairie, cattail or mixed emergent marsh.

Upland shrub and upland herbaceous (upland natural grass and upland planted grass) came from a map created at the first stage. In MLCCS, upland herbaceous primarily includes grassland with sparse trees, savanna, and mesic prairie. Therefore, conceptually, upland herbaceous is not equal to upland grassland. However, the upland grassland generated from the first-stage classification was used to represent the entire upland herbaceous class. This is acceptable since the number of savanna and mesic prairie areas is relatively small compared to the grassland. To improve the classification accuracy, post-classification refinement was performed by an image interpretation method that incorporated human experience, on-screen digitizing, AOIs and functionality of ERDAS Imagine, and used the MLCCS field data and DOQs as references.

3.2.3 Generation of Level 2-3 Urban (Percent Impervious Surface) Classes

Urban density is based on the percent of impervious surface. Impervious surfaces refer to any material that prevents the infiltration of water into the soil, such as streets and roads, parking lots, rooftops, sidewalks, and bedrock outcrops. The percentage of the land covered by impervious surfaces increases as the development alters the natural landscape (Arnold and Gibbons, 1996).

There is a strong relationship between the Landsat spectral-radiometric response and the percent imperviousness determined from measurements from DOQs and aerial photography. In particular, the "tasseled cap greenness" transformation of the Landsat data referred was used as input to an imperviousness estimation model. Greenness is directly related to the amount of green vegetation present and inversely to the degree of imperviousness. Based on this relationship, a regression model was created and utilized to classify urban area into 0-100% imperviousness.

To construct the model, the tasseled cap transformation was first performed on the September image. Greenness is the second component of the transformation. Theoretically, a similar amount of vegetation will have the same greenness value whether the background is dark (e.g., asphalt) or bright (e.g., concrete). Then, AOI samples with varying amounts of imperviousness, which were well distributed across the TCMA, were selected using the DOQs as the main reference. The percent imperviousness for each AOI was determined by digitizing the impervious area and then calculating the percent impervious for that AOI. A sample of 60, well distributed, AOIs representing varying percentages of impervious surface area were selected. Next, the mean greenness value for each AOI was calculated. Subsequently, a second-order polynomial equation was computed by fitting the sample data of the percent impervious and the mean greenness (Figure 3).

The R^2 value was 0.91, indicating a strong relationship and that most (91%) of the variation in imperviousness is accounted for by the variation in greenness. After this, the polynomial equation was entered into the spatial modeler in ERDAS Imagine, which used the greenness map of the tasseled cap transformation as the input image to estimate the impervious percentage. Finally, the urban mask from the first stage classification map was used to separate impervious surfaces from the bare soil, which have greenness values similar to impervious surfaces.

3.3. Third Stage – Final Map Generation and Post-processing

The Level-3 classification map was generated by combining all of the information classes from stage-1 and stage-2. It includes 0-100% impervious classes, cropland, planted conifer, planted grass, lowland conifer, upland conifer, upland deciduous, lowland deciduous, upland shrub, lowland shrub, upland herbaceous, lowland herbaceous, and water. The Level-2 classification map was created by recoding the Level-3 map into classes of 0-4% impervious, 5-10% impervious, 11-25% impervious

(low density urban), 26-50% impervious (medium density urban), 51-75% impervious (high density urban), 76-100% impervious (maximum density urban), cropland, planted trees and grass, coniferous, deciduous, upland shrubland and herbaceous, lowland shrubland and herbaceous, and water. The Level-1 classification map was recoded from the Level-2 map. It includes five classes: urban, cultivated, forest, nonforested natural area, and water as listed in the classification scheme.

Single, isolated pixels that produced a salt-and-pepper effect in the classified map were removed in a post-processing step. Since filtering affects the entire image and can alter the boundaries of the larger homogeneous areas, a different technique – elimination – was utilized. In this case, the isolated pixels were merged into the class that contributed to the majority of the polygon around the pixel.

4. Results

The final Level-3 classification map is shown in Figure 4 and the area statistics of the classifications are summarized in Table 3. The results show that urban and croplands dominate this area. For instance, approximately 36% of the total land is urban and 34% of the total land is agriculture. In addition, more than 90% of the forest is deciduous. Only small amounts of the total land are occupied by coniferous, shrubland, and herbaceous classes. The resulting classification also provides a continuous range of impervious area from 0 – 100%. These results can be readily incorporated into a GIS for further analysis.

Accuracy assessment was performed using the accuracy polygons generated from the MLCCS data. The locations of the data for accuracy assessment were selected randomly. The number of test pixels was based on the proportion of total pixels classified for a given class. In other words, the overall accuracy was weighted by the number or proportion of pixels in each class. The overall accuracy and Kappa value of the Level-1 class were 95% and 93%, respectively. The overall accuracy and Kappa value of the Level-2 map was 89% and 85%, respectively. Producer's and user's accuracy for the Level-2 map are recorded in Table 4. The value of the indices in the accuracy tables demonstrate high accuracies were achieved for Level-1 and Level-2 maps, which also means the multi-stage hybrid classification method was appropriate for this study.

The major cause of classification errors is undoubtedly similarities in spectral response for particular land cover types. However, there were also two problems regarding the ground truth data. First, some classes were not present and others had only a small number of ground truth polygons and/or the polygon sizes were quite small. The average polygon size was 38,500 square meters or approximately 42 Landsat pixels. However, many of the classes had only a small number of polygons larger than the width of the Landsat pixels. All of these conditions lead to problems. When only a small number of polygons are available to represent a class, it is less likely, given the inherent

variation within classes, to fully or adequately represent the class. And, if polygons are too small, they cannot be used because, in relation to the Landsat data resolution, they are mixed pixels that include responses from an adjacent cover type. Second, the ground data polygons were not evenly distributed in the study area. About 60% of ground data were located in Dakota County, and 20% were along the Mississippi River and Minnesota River. The other six counties contained only about 20% of the total ground data polygons. The unevenly distributed ground data might have affected our determination of classification accuracy.

Table 3: Statistics of the 2000 Landsat TCMA land cover classification.

Land Cover Class	Area (Hectares)	Area (%)
1-4% impervious	12,326	1.6
5-10% minimum density	8,065	1.0
11-25% low density	53,980	7.0
26-50% medium density	122,064	15.9
51-75% high density	53,324	6.9
76-100% maximum density	26,722	3.5
Cropland	263,365	34.2
Planted trees	6,072	0.8
Planted grasses	5,687	0.7
Upland conifer	70	0.0
Lowland conifer	2,877	0.4
Upland deciduous	74,842	9.7
Lowland deciduous	12,431	1.6
Upland shrubland	5,616	0.7
Lowland shrubland	7,835	1.0
Upland herbaceous	13,475	1.8
Lowland herbaceous	55,105	7.2
Water	46,028	6.0
Total	769,884	

Table 4: Accuracy assessment results of the 2000 TCMA classification.

Land Cover Classification	Producer's Accuracy (%)	User's Accuracy (%)
Urban (1-100% impervious)	95	97
Cultivated cropland	93	95
Planted trees & grasses	91	51
Coniferous	63	40
Deciduous	96	82
Upland shrubland & upland herbaceous	98	54
Lowland shrubland & lowland herbaceous	96	88
Water	99	97
Overall accuracy of Level-1 classification is 95% with Kappa equal to 93% Overall accuracy of Level-2 classification is 89% with Kappa equal to 85%		

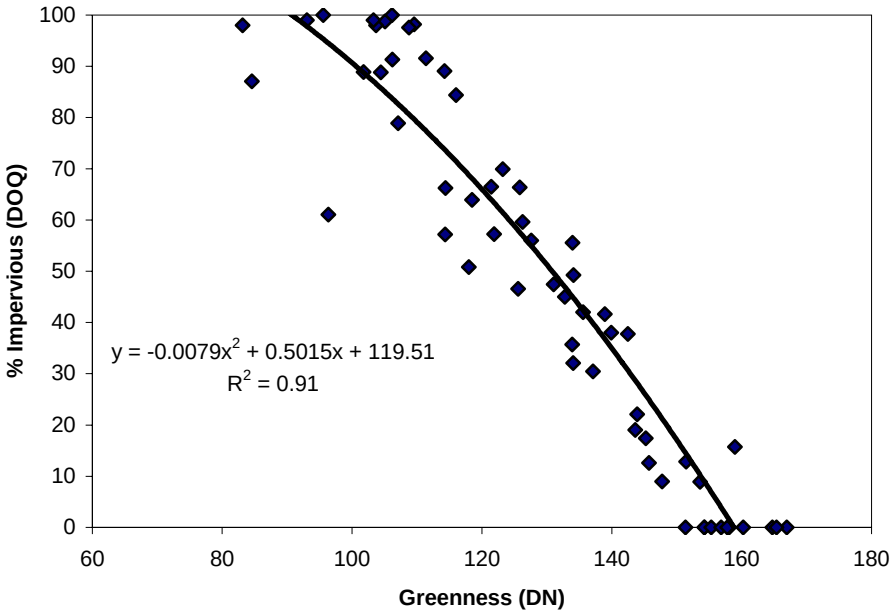

Figure 3. Relationship of greenness and percent impervious surface.

Additionally, the accuracy of the percent imperviousness in Level-3 map was tested by comparing the measurements from DOQs to the Landsat estimates. Figure 5 indicates there is a strong agreement (R^2 = 0.96) and standard error of 8.1 between the percent imperviousness from the statistical model based on TM data and the measurements from DOQs.

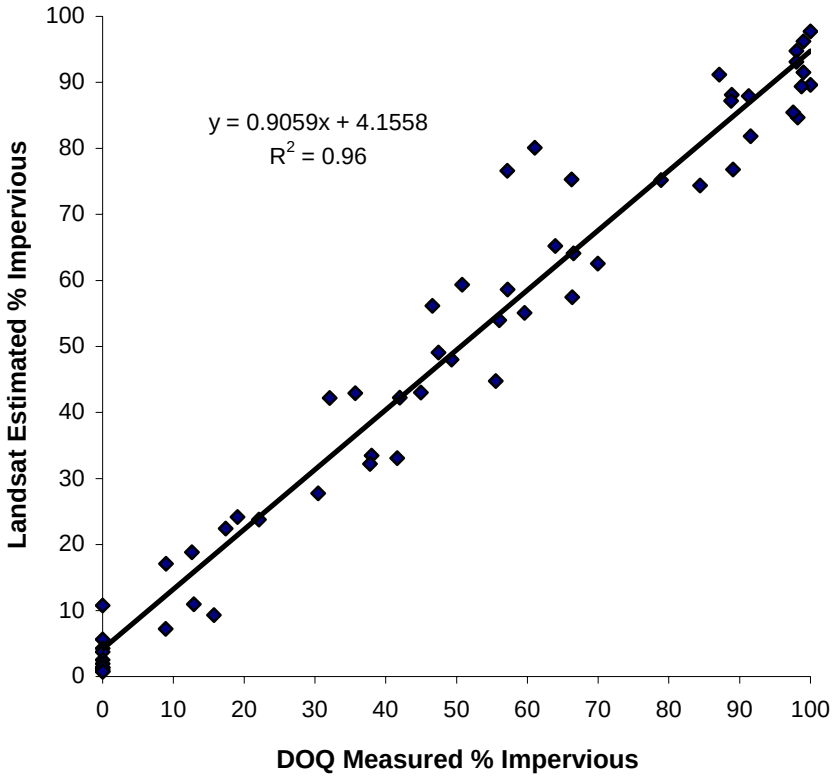

Figure 5. Accuracy of the percent imperviousness in Level-3 classification map tested by comparison of measurements from DOQs and the Landsat TM estimates.

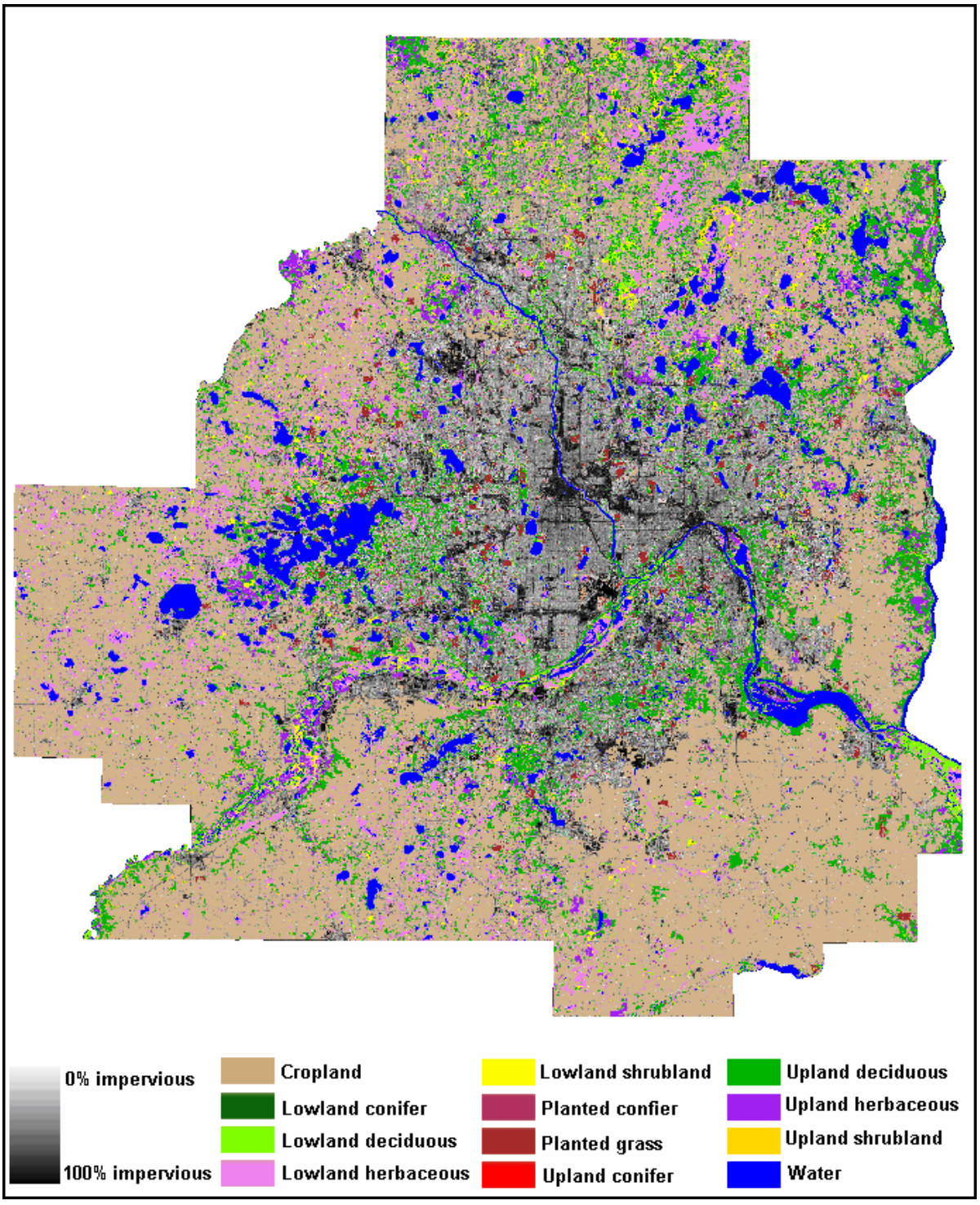

Figure 4. Level-3 land cover map of the Twin cities Metropolitan Area from classification of multi-temporal Landsat data of 2000.

5. Summary

In this study, multi-temporal Landsat TM and ETM+ digital imagery were used to classify land cover in the seven-county Twin Cities Metropolitan Area into three levels. High overall classification accuracy was achieved using the three-date TM data from different seasons by limiting the confusion between cropland and other vegetation types to a low and acceptable degree. Ancillary data were essential in helping to discriminate classes that are difficult to classify using only remotely sensed data. However, difficulties still exist with the three-date TM data. For example, we found it was difficult to define mixed forest and classify it with acceptable accuracy.

A multi-stage hybrid classification was performed. The multi-stage classification procedure was both conceptually and operationally explicit. High accuracy of the first stage classification and stratification is the key to successive Level-2 and Level-3 classifications. The urban and non-urban, forest and non-forest masks were critical for the next stages of classification. The statistical estimation model proved to be well suited for the classification of percent imperviousness. The theory based on the relationship between the amount of green vegetation present and the degree of imperviousness is simple and the procedure is replicable. The digital format of the classifications makes it possible to easily include them with other digital maps in a Geographic Information System for further analysis and modeling, while the Landsat imagery provides a synoptic view of the entire area.

Acknowledgement

This research was supported by Minnesota Metropolitan Council (contract SG-01-69) and field data were provided by Minnesota Department of Natural Resource. Additional support was provided by the University of Minnesota, Agricultural Experiment Station, project 42-037.

References

Anderson, J.R., E.E. Hardy, J.T. Roach, and W.E. Witmer, 1976. A land use and land cover classification system for use with remote sensing data. USGS Professional Paper 964, U.S. Geological Survey, Reston, Virginia.

Arnold, C. and J. Gibbons, 1996. Impervious surface coverage: the emergence of a key environmental indicator. Journal of the American Planning Association, 62(2): 243-258.

Bauer, M.E, C.A. Sersland, and S.J. Steinberg, 1996. Land cover classification of the twin cities metropolitan area with Landsat TM data. Proceedings Pecora 13 Symposium, Sioux Falls, SD, August 20-22, pp 138-145.

Bauer, M.E., T.E. Burk, A.R. Ek, P.R. Coppin, S.D. Lime, and T.A. Walsh et al., 1994. Satellite inventory of Minnesota forest resources. Photogrammetric Engineering and Remote Sensing, 60(3): 287-298.

Bauer, M.E., N.J. Heinert, J.K. Doyle, and F. Yuan, 2004. Impervious surface mapping and change monitoring using satellite remote sensing. Proceedings, American Society of Photogrammetry and Remote Sensing Annual Conference. Denver, Colorado, May 24-28, 2004, unpaginated CD ROM, 10 pp. In Press.

Benson, A.S. and S.D. DeGloria, 1985. Interpretation of Landsat-4 Thematic Mapper and Multispectral Scanner data for forest surveys. Photogrammetric Engineering and Remote Sensing, 51(9): 1281-1289.

Brown, J, T. Loveland, J. Merchant, B. Reed, and D. Ohlen, 1993. Using multisource date in global land cover characterization: concepts, requirements, and methods. Photogrammetric Engineering & Remote Sensing, 59:977-987.

Coppin, P.R. and M.E. Bauer, 1994. Processing of multitemporal Landsat TM imagery to optimize extraction of forest cover change features, IEEE Transactions on Geoscience and Remote Sensing, 32(4): 918-927.

Foody, G.M., 1995. Land cover classification by an artificial neural network with ancillary information. International Journal of Geographic Information Systems, 9(5): 527-542.

Lunetta R.S., J. Ediriwickrema, D.M. Johnson, J.G. Lyon, & A. McKerrow, 2002. Impacts of vegetation dynamics on the identification of land-cover change in a biologically complex community in North Carolina, USA. Remote Sensing of Environment, 82: 258-270.

Ma, Z., H.M. Melissa, and R.L. Redmond, 2001. Mapping vegetation across large geographic areas: Integrating remote sensing and GIS to classify multisource data. Photogrammetric Engineering & Remote Sensing, 67(3): 295-308.

McIver, D.K. and M.A. Friedl, 2002. Using prior probabilities in decision-tree classification of remotely sensed data. Remote Sensing of Environment, 81: 253-261.

Mumby P.J. and A.J. Edwards, 2002. Mapping marine environments with IKONOS imagery: enhanced spatial resolution can deliver greater thematic accuracy. Remote Sensing of Environment, 82: 248-257.

Nelson, R., R. Latty, and G. Mott, 1984. Classifying northern forests using Thematic Mapper simulator data. Photogrammetric Engineering & Remote Sensing, 50(5): 607-617.

Özesmi, S. L., 2000. Satellite remote sensing of wetlands and a comparison of classification techniques. Ph.D. Thesis, University of Minnesota, St. Paul. Minnesota. 220 pp.

Reese, H. M., T.M. Lillesand, D.E. Nagel, J.S. Stewart, R.A. Goldmann, and T.E. Simmons et al., 2002. Statewide land cover derived from multiseasonal Landsat TM data a retrospective of the WISCLAND project. Remote Sensing of Environment, 82(2):224-237.

Sawaya, K., F. Yuan and M. Bauer, 2001. Monitoring landscape change with Landsat classifications. Proceedings, American Society of Photogrammetry and Remote

Sensing Annual Conference, April 23-27, 2001, St. Louis, Missouri. Unpaginated CD, 10 pp.

Stefanov, W.L., M.S. Ramsey, and P.R Christensen, 2001. Monitoring urban land cover change: An expert system approach to land cover classification of semiarid to arid urban centers. Remote Sensing of.Environment. 77(2): 173-185.

Stuckens, J., P.R. Coppin, and M.E. Bauer, 2000. Integrating contextual information with per-pixel classification for improved land cover classification. Remote Sensing of Environment, 71(3):282-296.

Turner II, B.L., D. L. Skole, S. Sanderson, G. Fisher, L.O. Fresco, and R. Leemans, 1995. Land-use and land-cover change. Science/Research Plan. Stockholm and Geneva: IGBP Report No.35 and HDP Report No. 7.

Welch, R., 1982. Spatial resolution requirements for urban studies. International Journal of Remote Sensing, 3(2): 139-146.

Wolter, P.T., D.J. Mladenoff, G.E. Host, and T.R. Crow, 1995. Improved forest classification in the Northern Lakes States Using multi-temporal Landsat imagery. Photogrammetric Engineering and Remote Sensing, 61(9): 1129-1143.

Wright, H.E., Jr., 1972. Physiography of Minnesota. *In* P.K.Sims and G.B. Morey, eds. Geology of Minnesota, Minnesota Geological Survey, St.Paul, Minnesota. pp 561-578.